ELSEVIER

Journal of Nuclear Materials 270 (1999) 21–38

journal of nuclear materials

Fission product release mechanisms during reactor accident conditions

F.C. Iglesias [a], B.J. Lewis [b,*], P.J. Reid [c], P. Elder [d,1]

[a] *Ontario Hydro, 700 University Avenue, Toronto, Ont., Canada M5G 1X6*
[b] *Royal Military College of Canada, P.O. Box 17000 Stn Forces, Kinston, Ont., Canada K7K 7B4*
[c] *ALARA Research, Inc., 975 First Avenue, Saint John, New Brunswick, Canada E2M 4N9*
[d] *Atomic Energy of Canada Limited, Chalk River, Ont., Canada K0J 1J0*

Received 29 April 1998; accepted 22 July 1998

Abstract

During postulated accidents the reactor fuel is estimated to be exposed to a variety of conditions. These conditions are dynamic and, during the course of an accident, the fuel may experience a wide range of temperatures and conditions from highly oxidizing to mildly reducing environments. The exposure of the reactor fuel to these environments and temperatures may affect its stoichiometry and release performance. In this paper a review of the important fission product release mechanisms is presented. The results of three out-of-pile experimental programs are also summarized. © 1999 Elsevier Science B.V. All rights reserved.

1. Introduction

During postulated accidents the reactor fuel may experience a variety of atmospheric conditions. These conditions are dynamic and, during the course of an accident, the fuel could be exposed to temperatures ranging between 600°C and 2400°C and from highly oxidizing to mildly reducing environments.

The exposure of fuel to these environments and temperatures will affect its release performance. For example, the exposure of fuel to oxidizing environments will increase the oxygen potential of the fuel after the Zircaloy sheath is totally oxidized. As a result, the fuel stoichiometry will increase, changing its thermal and material properties. This stoichiometric modification will also have an effect on the fission product chemical speciation and consequently, the release characteristics.

In reducing environments, due to the low oxygen concentration in the coolant, the Zircaloy sheath may extract oxygen from the UO_2. This attack will produce a reduction in the fuel stoichiometry that will also affect the fuel thermal-mechanical properties and fission product speciation.

In the assessment of the source term to containment, individual release calculations for about 800 fission product and actinide radionuclides are not practical. This is due in part to the significant amount of computer time needed for a full core analysis. Since many isotopes have similar release characteristics, the concept of fission product release groups has been used in safety analysis for more than 20 yr to reduce necessary computation requirements. In order to develop these fission-product groupings, an understanding of the dominant release mechanisms is required.

Several experimental in-pile and out-of-pile research programs are actively studying the fission product release characteristics for all observable fission products. These programs provide evidence of the release characteristics of certain fission products and help in the integration of release groups. Also, equilibrium thermodynamic calculations are very powerful tools in the assessment of the most likely

---

[*] Corresponding author. Tel.: +1-613 541 6611; fax: +1-613 542 9489; e-mail: lewis_b@rmc.ca.

[1] Present address: Atomic Energy Control Board, P.O. Box 1046, Station B, Ottawa, Canada K1P 5S9.

PII: S0022-3115(98)00738-7

chemical speciation and consequently, in the expected release behaviour.

A review of the important governing fission product release mechanisms is given in Section 2. Section 3 describes the test facilities and summarizes the results of three out-of-pile experimental programs.

2. Fission product release mechanisms

2.1. Diffusion in fuel matrix

The intrinsic mobility will depend on the charge state of the atomic species that migrates by volume diffusion through the lattice of the fuel. When fission product atoms reach a free surface they may form thermodynamically favoured compounds. The chemical form will determine the subsequent gas-phase mass transport (i.e., vaporization). The mobility in the fuel is also determined by the solubility of the fission product in the UO_2 lattice. In oxide fuels, the chemical state can be typically grouped as: volatile fission products (Kr, Xe, Br, I); metallic precipitates (alloys) (Mo, Tc, Ru, Rh, Pd, Ag, Cd, In, Sn, Sb, Te); ceramic precipitates (oxides) (Rb, Cs, Ba, Zr, Nb, Mo, Te); and oxides dissolved in the fuel (Sr, Zr, Nb, Y, La, Ce, Pr, Nd, Pm, Sm) [1]. During irradiation, the noble gases are distributed dynamically between a fission-induced solution within the oxide lattice and their precipitation into intragranular and intergranular bubbles.

The release of short-lived fission gases from uranium dioxide during irradiation has been extensively studied in a number of experiments with single and polycrystalline fuel specimens, [2–5] and with swept assemblies in which the fuel-to-sheath gap of an intact operating fuel element was continually purged [6–9]. These experiments generally demonstrate that diffusion of noble gas atoms and iodine in UO_2 is the rate-determining mechanism for release during steady-state operation. At lower fuel temperatures ($<1000°C$) diffusion is independent of temperature (athermal) but is enhanced as a result of the fission process [4,10]; however, for the short-lived isotopes, recoil effects can also become important [11,12]. As shown in these various experiments, the diffusion coefficients of krypton, xenon and iodine were found to be similar in magnitude and in their temperature dependent behaviour. Both thermally activated and athermal diffusion are implicated as the main release mechanisms in these studies since the release-to-birth rate (R/B) ratio is observed to vary inversely as the square root of the decay constant. This type of behaviour was predicted over 30 yr ago by Booth using diffusion theory [13–15].

When the fuel rod becomes defective during transient conditions, an increase in the oxygen-to-uranium (O/U) ratio results in the direct enhancement of the diffusional release of fission products from the fuel matrix [16–20]. Experimental work has indicated that xenon diffusion occurs as a neutral tri-vacancy in uranium dioxide, [19] in agreement with the theoretical calculations of Grimes and Catlow [21]. These calculations also indicate that in hyperstoichiometric fuel (UO_{2+x}), the most stable solution site is the uranium vacancy [21]. This finding supports the model of Killeen and Turnbull for the noble gas diffusion coefficient in UO_{2+x} (for x in the range of 0.005–0.1), where it has been assumed that the gas atom mobility is influenced by the presence of the uranium cation vacancies in which Frenkel and Schottky equilibria govern the isolated point defects [20]. Specifically, since the anion Frenkel defects predominate in urania, an increase in the oxygen interstitial concentration results in a reduction of the oxygen vacancy concentration; however, due to the secondary Schottky equilibrium, an increased uranium vacancy concentration results. This model for the diffusion coefficient is in agreement with annealing test results in CO/CO_2, and with the experimental work of Lindner and Matzke [16,20]. The model is not in agreement, however, with the data of Miekeley and Felix where the diffusivity is not observed to continuously increase with the stoichiometry deviation [17]. The inconsistencies in the experiments of Lindner and Matzke versus those of Miekeley and Felix may be related to their relative antiquity [19]. The model has been used to describe the in-pile steady-state release of fission gas from defective fuel rods [22]. This treatment has also been successful in describing the cesium release kinetics in out-of-pile experiments conducted at high temperature in steam (see Section 2.5.4); i.e., a reduced release from Zircaloy-clad fuel specimens, compared to that with bare fuel fragments, can be attributed to limited fuel oxidation, arising from a lower oxygen potential due to hydrogen production from metal–water reaction [23,24].

A diffusional release of volatile fission products (e.g., Kr, Xe, I, Cs, Te) has been observed in a number of high-temperature, post-irradiation, annealing experiments with trace-irradiated polycrystalline UO_2 fuel samples [25], and high-burnup specimens taken from commercial spent fuel rods [24,26–34]. In an annealing experiment with spent fuel that was conducted in a hydrogen atmosphere, the measured release kinetics (and hence diffusivities) of I, Cs and Ba were similar; in a steam test, where the Zircaloy cladding had been completely oxidized, similar release kinetics were observed for I, Cs, Xe and Te [35]. This behaviour suggests that under the given conditions these species have similar solid-state diffusivities in the fuel matrix. Furthermore, this observation points to an additional mechanism in the role that the noble gases play in creating a network of interconnected porosity through which other fission products such as Cs, Te and I can escape to the free surfaces of the fuel [36].

An idealized model originally introduced by Booth [37] has been used extensively to interpret the diffusive release of the more volatile fission products in these post-irradiation annealing experiments. A square-root behaviour is theoretically predicted for the release fraction as a function of the anneal time. The equivalent-sphere model has been extended for a non-uniform distribution that develops in the fuel grains during the irradiation period when the fuel temperature is sufficiently high to allow for diffusion to occur [38]. The model has also been generalized to account for a time-dependent diffusivity that may arise from changing temperature and fuel stoichiometry conditions [24,29,34]. Several empirical models, based on a diffusion treatment and annealing test data, have been developed for source-term analysis [29,34,39–42]. However, in many out-of-pile experiments, the release kinetics are found to be much more rapid than that expected from diffusion theory alone; for example, enhanced kinetics, observed during temperature ramp-up, may result from a release of the stored inventory on the grain boundaries (see Section 2.3) [24,30–32,43]. Following this initial release, a slower diffusional component is typically observed. More mechanistic treatments have also been developed to assess the distribution of fission products in the fuel, and the amount of their release, by considering the combined effects of fission product generation, atomic migration, bubble nucleation and resolution, bubble migration and coalescence, channel formation on grain faces, interlinking on grain edges, and microcracking [36,44–47].

Experiments to study the release behaviour of Te, I, Ru, Mo and Xe in hyperstoichiometric sintered fuel specimens have been carried out under trace-irradiation conditions [48]. In this case, significant grain growth occurred because of the greatly enhanced uranium ion diffusivity in UO_{2+x}, which supplements intragranular diffusion as a means of delivering fission products to the grain boundaries. In contrast, with high-burnup fuel, grain growth is not an important fission product release mechanism because of the pinning of the grain boundaries by the fission product bubbles [23,24,39,49–52]. On the other hand, some interpretative analysis suggests that a grain growth/grain-boundary-sweeping mechanism is responsible for a relatively large intragranular fission product release in the Horizontal Induction (HI) series of high-burnup fuel tests (i.e., HI-1, HI-2, HI-3 and HI-4) conducted at the Oak Ridge National Laboratory (ORNL) (see Section 3.1) [45]. However, significant grain growth was not observed in more recent tests with higher-burnup fuel in the ORNL Vertical Induction (VI) experiments (see Section 3.1) as well as in the Heva/Vercors experiments at the Commissariat à l'Energie Atomique (CEA) (see Section 3.2) [29,40,41].

2.2. Fission product vaporization from fuel surfaces

The release kinetics of the volatile or relatively volatile fission products (Xe, Kr, Cs, I, Te, Sb) can be described by a rate-limiting process of solid-state diffusion through the UO_2 fuel matrix [29,35,42]. However, for non-volatile fission products (e.g., Sr, Y, Zr, Nb, Mo, Tc, Ru, Rh, Pd, Ba, La, Ce, Pr, Nd), their escape from free surfaces into the gas phase may be so difficult that surface or gas-phase transport processes can control the overall kinetics [25]. This rate-limiting step is related to the chemical state of the fission products (i.e., vapour pressure of the thermodynamically favoured compounds) that are formed at the fuel surface, and to the mass transfer from the free surface of the fuel to the bulk, hydrogen-steam, gas flow [35,39,42,53–56]. The chemical state of the fission products will depend on the temperature and oxygen potential of the gas environment. The oxygen potential can change as a result of hydrogen production from the steam oxidation of structural materials (Zircaloy) within the damaged core. The equilibrium chemical composition can be obtained (where thermodynamic data permit) by a minimization of the free energy for a multi-component system consisting of a condensed phase (i.e., fuel plus fission products) and a gas phase (steam, hydrogen and gaseous fission product species) [42,54–59]. The vapour species released into the bulk environment may, typically, be found in either an elemental/compound form, or as an oxide or hydroxide.

The chemical form of the fission product can significantly affect its volatility. The oxygen potentials required for the formation of fission product oxides, for example, can be obtained from an Ellingham diagram [1,35,57,60]. Here, the most stable oxides (e.g., CeO, and LaO) are formed at low oxygen potentials. Also quite stable are the oxides BaO, SrO and Eu_2O_3. On the other hand, oxides requiring relatively high oxygen potentials for formation include the species TeO_2, Sb_2O_3, and RuO_4. Consequently, for typical, high-temperature, reactor accident conditions (with atmospheric ratios of H_2/H_2O of ten to one-tenth), the La, Ce, Eu, Sr, and Ba fission products should be in the form of oxides, while the Ru, Te, and Sb fission products should be found as metals.

Small releases of Ba, Sr and Eu are therefore expected in a steam environment from the low-volatility oxides in the fuel. For example, in the Vertical Induction (VI) tests at the ORNL (see Section 3.1), small releases of Eu have been observed in steam ($<0.01\%$) [24,29]. Releases of Ba, Sr and Eu measured in the Severe Fuel Damage tests in the Power Burst Facility and Three Mile Island Unit 2 accident were also small (typically 1% or less) [60]. In contrast, much higher Eu releases (19–57%) were observed in the VI hydrogen tests, under similar temperature conditions, where higher-volatility metallics may have formed [24,29]. Similarly, in-pile measurements of fission product releases in the ST-1 and ST-2 hydrogen experiments at the Sandia National Laboratories indicate much higher Ba and Sr releases of several percent and up to 15% for Eu [60,61].

For the refractory metals, Ru and Mo, the oxides (RuO_4, and MoO_2) are much more volatile than the elements, so that high releases would be expected only under strongly oxidizing conditions (high oxygen potentials). In the VI-3 test (2700 K in steam) only 5% of the Ru was released from the fuel [29], while at 1600 K almost 100% of the Ru was released in experiments conducted in air at the Chalk River Laboratories (CRL) (see Section 3.3) following significant oxidation of bare fuel samples [62]. The observed Ru releases are consistent with thermodynamic arguments [42,63].

2.3. Fission product release during temperature ramps

In-pile power-ramp tests have produced greater gas (Xe and Kr) release than expected from a pure diffusion mechanism. The gas release rates are also higher than those measured during steady-state irradiations [64]. To assess the fuel behaviour and fission power release during power ramps and accident conditions, in which the fuel is subjected to fast temperature excursions, several experiments have been performed out-of-pile, in direct electric heating tests [65], with central line heating rates between 6°C/s and 76°C/s. It was concluded for heating rates higher than 50°C/s that the most probable mechanism of release was grain boundary separation. Significant releases from the grains were required to supply the grain boundaries with the required fission product inventories to match the observed releases. A comparison of the calculated versus observed results of the grain-boundary separation and transient gas release behaviour in the direct electrical heating tests is presented in the analysis of Ref. [44].

The results of Une and Kashibe [43,66,67], using an induction furnace, also point to a higher saturated grain boundary inventory (by a factor 2–4) in order to match the experimental results. During the heating phase of each experiment, a Kr burst was detected followed by a slower diffusional process. They interpreted their observed release as controlled by grain boundary bubble interconnection and tunnel formation. However, using fractographic techniques, they determined that up to heating rates of 10°C/s, no grain boundary separation was observed. This observation is in agreement with the results of Rest and Gehl [65]. Small et al. [68,69] have also studied the release during ramps between 1°C/s and 50°C/s, which indicates maximum release rates around 10°C/s.

A physical mechanism is needed to account for enhanced releases during temperature ramps. Phenomenological approaches can be adopted [70] until a more complete mechanistic model is available. This extra grain boundary inventory may be released by the standard grain boundary bubble interconnection for heating rates up to 10°C/s, or by grain boundary separation at higher heating rates. As most of the measurements were performed on Kr, no clear role has been attributed to other volatile fission products (Cs, I, Rb, Br). Also, no experimental information has been obtained about the release behaviour during temperature ramps on non-stoichiometric fuel.

2.4. Matrix stripping (fuel volatilization)

Alexander [71] has observed that in oxidizing environments at temperatures of 2100 K or higher, the volatilization of diverse species like Mo, Y, La and Ba exhibited the same activation energy for release. Neither the nature of the species nor the nature of the solid state in the UO_2 matrix showed a significant effect. Cox et al. [51] also reported significant weight loss of UO_2 in CRL experiments with steam after a certain period of time. Similar results were obtained in experiments at the Commissariat à l'Energie Atomique (CEA) [24]. The weight loss is observed to increase with increasing temperature. These two observations indicate a volatilization of uranium mass which, in turn, will result in a release of fission products from the fuel matrix.

If the Zircaloy sheath is severely oxidized, the oxidizing environment can react with UO_2 and, under these conditions, the UO_2 will incorporate excess oxygen to form hyperstoichiometric UO_{2+x} or be converted to a higher oxide. At temperatures above 1800 K, UO_{2+x} is the stable condensed phase in both air and steam. A significant vapour pressure of uranium bearing species is predicted at equilibrium. Since the gases in contact with the fuel do not constitute a closed system, the condensed phase is vaporized at a relatively rapid rate. As the matrix is volatilized, the remaining noble gases (Xe, Kr) and volatiles (Cs, I, Br, Rb) will be released from the volatilized fuel volume. The low volatility fission products that were previously inside the fuel matrix become concentrated at the fuel surface, where they will accumulate until they are vaporized (see Section 2.2) [42] or else entrained in the flowing gases as particulates. This mechanism of fission product release, which results from fuel volatilization, has been termed 'matrix stripping' [42,51,71–74].

UO_3 or $UO_2(OH)_2$ were identified as the most likely uranium-bearing species in the volatilization process. However, at high temperature and atmospheric pressure steam, UO_3 is the dominant uranium-bearing vapour, i.e., the partial pressure of $UO_2(OH)_2$ is only important at relatively low temperatures and for accident scenarios involving high steam pressures [75]. In the calculation of the UO_3 partial pressure, the effect of fuel burnup is much less significant than the uncertainty in the thermochemical data for the free energy of formation of $UO_3(g)$ [76–81]. For example, following a literature review of urania thermochemistry, the predicted equilibrium pressure of UO_3 over pure UO_{2+x} in a gas with a known oxygen potential cannot be estimated to better than one order of magnitude at 2000 K [75].

The process of fuel volatilization in steam has been modelled for incorporation into severe accident codes [42,76,82,83]. The vaporization rate is significantly overpredicted using the Hertz–Langmuir formalism for evaporation into a vacuum [72,76,83]. However, models based on conventional boundary-layer mass transfer have proven successful [42,82]. On the other hand, ceramographic examination of both irradiated and unirradiated samples exposed to air at high temperature showed that volatilization and pore growth occurs preferentially along some grain boundaries, while other boundaries do not participate as readily in the reaction [74]. This preferential reaction at localized sites indicates that perhaps a surface chemical reaction, rather than gas phase mass transfer, may be the rate-controlling process.

For the case of high-volatility fission products, in which the release process is controlled by diffusion through the fuel grains, the volatilization will decrease the time required for these fission products to reach the open surfaces. An instantaneous release of the volatile fission products contained in the volatilized UO_2 volume is supported by the observations.

In the case of the low-volatile fission products, for which the controlling process is vaporization from open surfaces (see Section 2.2), the volatilization process will increase the concentration of these fission products in the open surfaces. However, the effect of this increased concentration of low-volatile fission products on the uranium volatilization rate has not yet been determined.

2.5. Effects of zircaloy cladding

2.5.1. UO_2/zircaloy interaction

Uranium and zirconium can form an alloy. The melting point of the alloy varies with its composition, and can be as low as ~1150°C. This alloy can be formed through reduction of the UO_2 (to UO_{2-x} + U) by Zircaloy which is still in the solid phase.

With contact between Zircaloy and UO_2, a series of metallographic structures will develop [84–86], i.e., outward from the fuel pellet surface one observes: (i) a mixture of $Zr_\alpha(U)$ and (U,Zr); (ii) a layer of (U,Zr); (iii) a layer of $Zr_\alpha(O)$; and (iv) the remaining of the Zircaloy sheath. It has been shown that the presence of a CANLUB layer can inhibit the chemical attack of UO_2 by the Zircaloy [86]. In this process, some fuel 'liquefaction' may result in the fuel element, well below the melting point of UO_2. The occurrence of this liquefied material can contribute to an enhanced fission product release as a consequence of the fuel reduction. Liquefaction has been observed, for example, primarily along the grain boundaries during the ORNL HI-4 test (see Section 3.1) [87]. It is unclear if the concentration of fission products is a major contributor to this feature.

2.5.2. UO_2 dissolution by molten zircaloy

If fuel heatup in an accident is sufficient to produce molten Zircaloy, the Zircaloy can act to reduce the UO_2, producing a liquid (U,Zr)O + $(U,Zr)O_{2-x}$ mixture. The (U,Zr)O is a liquid at temperatures (~1150°C) which are significantly below the melting point of UO_2. This dissolution and liquefaction of the UO_2 matrix will result in large fission product release of all isotopes which either have a large partial pressure or which can form volatile compounds in the prevailing environment.

Many experiments have been carried out using unirradiated UO_2 to investigate this phenomenon. Hofmann et al. [84,88] and Nikolopoulos et al. [89] give the results of crucible experiments in argon for temperatures in the range 1800–2000°C. In these experiments, the chemical attack of the UO_2 was sufficient to disintegrate the crucibles. This large-scale chemical attack of the UO_2 by the Zircaloy required intimate contact between the fuel and the molten cladding for a period of > 100 s. This requirement is due to the fact that O-poor Zircaloy does not wet the UO_2. Therefore, the molten Zircaloy must be oxidized by the UO_2 before it can wet the UO_2, penetrate along cracks and over the entire available surface area and significantly affect the UO_2 morphology. Oxidation of the Zircaloy by the UO_2 occurs as quickly as oxidation of Zircaloy by steam, since the rate-limiting step is diffusion of the oxygen in the Zircaloy.

Kim et al. [90] report the results of experiments similar to those described above. These experiments confirm that the chemical attack of UO_2 by Zircaloy acts along exposed surfaces and cracks so that the wetting behaviour of the molten Zircaloy is important. The interaction therefore develops in layers for simple geometries, and the layer growth can be described using parabolic rate kinetics. These experiments also confirm the expected result that, while O-rich Zircaloy wets the UO_2, more completely, the dissolution rate is reduced due to the fact that the molten Zircaloy already contains some O and so the reaction with O from the UO_2 is less energetically favourable.

Rosinger et al. [91] and Hayward et al. [92–95] report experiments which are intended to more closely represent CANDU fuel. These experiments examine dissolution of unirradiated UO_2 by molten Zircaloy for temperatures of 1970–2500°C. These experiments indicate that, if heatup is slow enough (i.e., the Zircaloy oxidation is sufficient to allow it to wet the fuel element), the molten Zircaloy will not drip off of the fuel element and will then reduce the UO_2. The reduction of the UO_2 will dissolve a percentage of the fuel element which depends on the temperature of the melt and the initial oxygen content of the Zircaloy. These experiments indicate that O-free Zircaloy will dissolve ~60% more UO_2 than $Zr_\alpha(O)$ if it is able to wet the fuel.

Several models have been proposed to describe the experimental results of the various groups [96–100], although these models have been unable to resolve the inconsistencies in the different data. In particular, Hayward and George [92–95] observed a cessation of the UO_2 dissolution process during an initial saturation stage, whereas other groups experienced a continuation of dissolution in a second precipitation stage with a continuous increase of the ceramic phase portion in the refrozen melt [88,90]. However, a more general treatment, suggests that the different dissolution kinetics can be attributed to the relatively small dimensions of the crucibles used in the experiments of Hayward and George, and the different UO_2/Zircaloy mass ratios [101]. The theoretical description of the precipitation stage considered: (i) dissolution of the UO_2 crucible by the liquid phase; (ii) formation and growth of the ceramic (U, Zr)O_{2-x} precipitates; and (iii) diffusional transport of oxygen from the solid oxide to the liquid. Since the last process is particularly important as diffusion in the solid phases determine the kinetics of the other two processes, an improved measurement of the chemical diffusion coefficient of oxygen in UO_{2-x} has been made to firmly establish the concentration driving force [102].

Indications of dissolution of UO_2 by molten Zircaloy in fission product release experiments have been limited to experiments in reducing environments. This is due to the fact that, in oxidizing environments, experiments which have heated up to temperatures sufficient to melt Zircaloy in an oxidizing environment have heavily oxidized the Zircaloy cladding before reaching these high temperatures. ZrO_2 does not reduce UO_2. Only in experiments in which Zr or $Zr_\alpha(O)$ is present in significant quantities at the time of melting does significant UO_2 dissolution take place.

The ST-1 [103,104] and VI-4 [105] experiments were both LWR fuel experiments in which fuel was heated to 2400–2500 K in a H_2-rich gas flow. These experiments showed evidence of attack of UO_2 by molten Zircaloy and formation of the low melting point (U, Zr) eutectic. The attack was sufficient that macroscopic dissolution of the UO_2 matrix occurred. These processes occur at such high temperatures, however, that any additional fission product release is swamped by the already high release rate associated with high temperatures for volatile fission products and noble gases [24]. Release of non-volatiles did not seem to be affected, except in the case of Eu, which had its release enhanced, and Sb and Te, which were released in much lower amounts than would be expected in an oxidizing environment in which molten Zircaloy-UO_2 interaction does not take place. The reduced release of Sb and Te is not directly related to attack of the UO_2 by molten Zircaloy, but to the presence of metallic Zircaloy to react with (see Section 2.5.3). The enhanced release of Eu is attributed to the reducing chemical environment (see Section 2.2) and not to the attack of the UO_2 by molten Zircaloy.

A theoretical treatment based on bubble rise in a viscous liquid has been developed to account for the fuel dissolution effects on fission product release [24,36].

2.5.3. Zircaloy trapping effects

As fission product vapours are released from the fuel matrix and reach the fuel-to-clad gap, some of these species will chemically react with the inner surface of the Zircaloy cladding. For instance, chemical trapping of antimony, barium and tellurium have been observed in several annealing experiments [29,35,40,60,106]. For instance, tellurium and barium have been identified in the cladding material of the HEVA-6 fuel specimen following a post-test examination using a gamma-ray tomography technique [35,107]. The releases of antimony and tellurium are particularly dependent on the Zircaloy oxidation state, where releases of these species do not occur until the Zircaloy cladding is nearly completely oxidized. A number of experiments have also been performed to determine the chemical form of the tellurium during reaction with the Zircaloy cladding prior to and following Zircaloy oxidation [108–111].

In the Zircaloy oxidation experiments of de Boer and Cordfunke [111], a thin band of tin was found segregated in the zirconium oxide layer due to the lower solid solubility of tin in the oxide compared to the metal. This band was found to move towards the inner surface of the cladding with the advancing metal/oxide interface as the oxide layer became more stoichiometric. From additional tellurium/Zircaloy reaction experiments [111], after complete clad oxidation, a release of tellurium is observed to occur due to the production of elemental tellurium and zirconium oxide from reaction of zirconium telluride with oxygen. However, due to the tin segregation process, there is an enhancement for the formation of tin telluride (SnTe), where a thermodynamic analysis indicates that SnTe will form provided that the oxygen potential is below the equilibrium value for the formation of SnO_2 and tellurium [111]. In fact, for typical reactor accident conditions, SnTe will be the predominant compound of tellurium release from Zircaloy clad fuel as observed, for example, by Collins et al. [106] Only at high oxygen pressures that are above the equilibrium value of Sn/SnO_2 will tellurium be released in its elemental form.

2.5.4. Gap transport, oxygen potential and hydrogen absorption effects

During a high-temperature reactor transient, with a continuous diffusive release of fission gas from the fuel matrix into the fuel-to-clad gap, and a possible reduced primary coolant pressure due to coolant blowdown, a pressure differential may result between the gap and the primary coolant in a defective rod [112,113]. This pressure differential can lead to an important bulk-convective flow which will enhance the fission-product vapour transport in the gap. In this case, for the short-lived isotopes, significant decay will no longer occur during transport in the gap [112,113].

For fuel oxidation to occur, steam must diffuse into the breached rod against any counter-current flow of non-condensable fission gases, and out-flowing hydrogen that is produced from the internal reaction of the incoming steam with the Zircaloy cladding or urania [114–116]. As such, it is important to determine the local hydrogen-to-steam molar ratio (i.e., oxygen potential) along the gap as this ratio directly affects the fuel oxidation state. The fuel oxidation state, in turn, significantly influences the rate of fission-product diffusion in the fuel matrix and the subsequent release into the gap (see Section 2.1). The oxygen potential in the gap will also affect the chemical form of the fission product, which will dictate the amount of vaporization of low-volatile products from the fuel surface (see Section 2.2). For instance, the fission product release kinetics were observed to differ in CRL annealing experiments conducted at high temperature in steam with bare fuel fragments versus mini-elements (i.e., short-length Zircaloy-clad fuel specimens) (see Section 3.3) [117]. While the Zircaloy clad is oxidizing, the oxygen potential in the bulk atmosphere will be significantly reduced due to hydrogen production from the Zircaloy/steam reaction, leading to a decreased volatile (cesium) release [23,24]. Even after the Zircaloy sheath has been completely oxidized, the release kinetics are reduced due to limited transport in the gap and a lower oxygen potential as a result of inhibited steam penetration into the gap of the mini-elements.

Parabolic kinetics have generally been used to model the Zircaloy oxidation process for estimation of the oxygen potential in the bulk atmosphere [76]. This simple parabolic approach may not be satisfactory since: (i) the parabolic kinetic theory is only strictly valid for a semi-infinite medium; (ii) their may be a rate limitation due to gas-phase mass transport of steam from the bulk gas to the gas/oxide surface; (iii) the oxide scale may in fact shrink due to dissolution in the remaining metal (leading to exposure of the bare metal to a hydrogen-rich gas); and (iv) without an outer protective oxide layer, hydrogen absorption by the metal can take place [115,118–121]. The last three processes will occur in steam-starved conditions (i.e., steam–hydrogen mixtures). The limitations of the parabolic model can be removed by treating the Zircaloy corrosion process as a moving-boundary diffusion phenomenon [118–121]. When the oxide scale disappears due to steam starvation of the gas, hydrogen can rapidly saturate the metal, resulting in a removal of hydrogen from the bulk gas flow. The dissolved hydrogen may influence the subsequent oxidation kinetics of the metal. In addition, hydrogen uptake in the cladding will release heat, i.e., at a total system pressure of 1 atm, H_2 dissolution in the metal will only augment the heat release by ~5% whereas, at 50 atm, this effect is much more pronounced where the heat release is about ~1/3 that due to steam corrosion [118]. This additional heat will of course enhance any temperature-dependent fission product release processes.

2.6. UO_2 melting

At sufficiently high temperatures, UO_2 melts. Stoichiometric UO_2 melts congruently at a unique temperature [122], but hypo- or hyper-stoichiometric UO_2 does not and has separate solidus and liquidus temperatures. Latta and Fryxell [123] have determined the solidus and liquidus lines for UO_{2+x} experimentally. Non-stoichiometric UO_2 has solidus and liquidus lines which are lower in temperature than the congruent melting point of $UO_{2.00}$ and a monotectic forms at an O/U ratio of ~1.65, with a melting point of ~2425°C. Their experimental data extends to $UO_{2.23}$, which allows reasonable extrapolation to $UO_{2.25}$. The solidus/liquidus lines are as shown in Fig. 1, along with the high temperature U–O phase diagram.

The solidus and liquidus lines are also affected by the presence of fission products which are produced in the UO_2 as burnup increases. These fission products can be grouped into three broad classes. In the first, the fission products are insoluble in either solid or liquid UO_2. Since these fission products do not interact with the UO_2 in any way, they do not affect the melting point. Examples of these fission products are Cs, I, Kr and Xe, as they all behave as gases diffusing through the fuel matrix, as well as noble metals such as Mo, Rh, Ru, etc., which are present in power reactor fuel as metallic precipitates which do not interact with the fuel matrix.

The second class of fission products are materials, such as Sr and Ba, which are soluble in the liquid phase and are hence able to form eutectic alloys. Adamson [124] assessed this impact on melting temperatures using data from Koizumi et al. [125] and Boyle et al. [126]. The estimated decrease in UO_2 melting temperature is <5 K at 225 MWh/kgU and ~12 K at 700 MWh/kgU. Hence it can be concluded that there is no significant impact on the fuel melting temperature due to the influence of eutectic-forming fission products. However, the presence of these fission products does complicate the assessment of UO_2 melting by metallographic examination, since they can cause features such as rounded grains, which can be misinterpreted as indications of the onset of melting.

The third class of fission product which can affect the melting behaviour of UO_2 includes the actinide oxides,

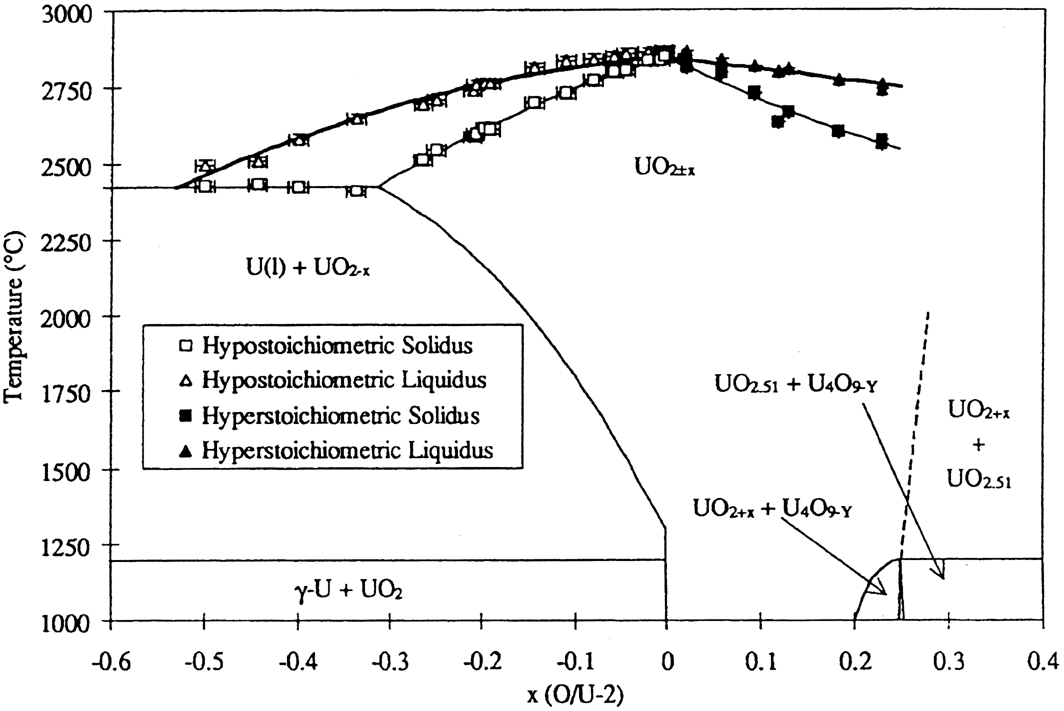

Fig. 1. High temperature O–U phase diagram showing measurements of solidus and liquidus lines by Latta and Fryxell.

rare earth oxides and Zr. The element in this class which is produced in the greatest quantities in CANDU fuel is Pu. The impact of Pu on the solidus and liquidus lines can be assessed [127] using the assumption of an ideal solution. Using this, in conjunction with experimental data, the effect on the solidus and liquidus lines can be estimated. This effect results in a decrease in the melting temperature of <5 K for CANDU fuel at a burnup of 700 MWh/kgU.

Assessment of the impact of fission products produced as a function of burnup indicates that they have a much smaller effect than changes in stoichiometry. The effect at a burnup of 700 MWh/kgU is <17 K. At more usual burnups for CANDU fuel, the impact is <3 K.

When the UO_2 melts, fission product release is very similar to the case of UO_2/Zircaloy interaction (see Section 2.5.1) or UO_2 dissolution by molten Zircaloy (see Section 2.5.2). Any fission products which are volatile or whose chemistry is such that, in the prevailing environment, they can form a volatile compound, will be released. Other fission products will be released based upon their vapour pressure at that temperature.

2.7. *Fuel frothing*

In Section 2.5, various processes were described which ‘liquefy’ the UO_2 that is, they result in a significant disruption of the UO_2 matrix. This will lead to a release of fission gases and volatile fission products, which are retained in the fuel matrix at the time of ‘liquefaction’.

The pressure of fission gases and highly volatile fission products in the intact fuel matrix can be very high. If the matrix is suddenly disrupted, these fission products can form large bubbles since the restraint of the UO_2 matrix is no longer available to restrict the fission product volume. This process results in a large increase in the volume of the fuel, a phenomenon which is referred to as either ‘fuel frothing’ or ‘fuel foaming’ [128].

Fuel frothing has been observed in experiments with irradiated fuel in which the fuel has been liquefied either by melting or by dissolution of UO_2 by molten Zircaloy. The amount of UO_2 affected by the UO_2/Zircaloy solid state interaction (see Section 2.5.1) is sufficiently small that fuel frothing does not occur. Dissolution of UO_2 by molten Zircaloy (see Section 2.5.2) has been observed in significant quantities in tests in a reducing environment, such as ST-1 [103,104] and VI-4 [105], since these tests had significant amounts of non-oxidized Zircaloy available to wet the UO_2 at temperatures above the Zircaloy melting point. Most experiments which heat up to such high temperatures in an oxidizing environment do not result in fuel frothing [129], since these tests are of long duration and the Zircaloy is fully oxidized by the time the melting temperature is reached.

An exception to this general trend is BTF-107 [130]. In this test, a flow blockage occurred which resulted in rapid temperature escalation for the fuel sheath to temperatures well in excess of the Zircaloy melting point. The escalation was sufficiently rapid that the Zircaloy was not fully oxidized before reaching the melting temperature. Therefore, molten metallic Zircaloy was available to wet the UO_2 and reduce it to UO_{2-x}. Post-test examination of the fuel shows that the molten Zircaloy wetted the UO_2 along all exposed surfaces, including the cracks, and formed the molten (U, Zr)O eutectic phase. Large-scale dissolution of the UO_2 matrix appears to have occurred, resulting in fuel frothing.

Because of the smaller fission gas production in the relatively low burnup CANDU-type fuel used in BTF-107, the amount of fuel frothing was less in BTF-107 than in ST-1 and VI-4. The volume expansion in BTF-107 can be estimated at $\sim$10%, as compared to 50–100% in the higher burnup LWR experiments. As would be expected in CANDU fuel, this is due to the lower gas quantity generated in the fuel matrix during irradiation.

Fuel frothing is a mechanism whereby a small amount of highly volatile fission products can be retained in the fuel, trapped in the bubbles. At these high temperatures, most of the volatile fission products would be released even in an oxidizing or inert environment, so the dissolution of the fuel matrix does not have as large an effect on fission product release as would initially be expected. However, the volume increase associated with fuel frothing could have an impact on the accessibility of coolant to the fuel, which could result in more severe temperature transients than would be the case if frothing did not occur. These higher temperatures could also have a feedback effect on fission product releases. Therefore, it is important that this process be considered in accident scenarios in which it is possible for Zircaloy to exceed its melting temperature of 1760°C. A theoretical analysis of the UO_2 foaming potential was developed based on an assessment of the time characteristics for bubble growth, surface escape, film thinning and bubble coalescence, i.e., this analysis suggests that the foams are relatively unstable and tend to collapse with a release of the volatilized fission products from the molten fuel debris [128].

3. Experimental database

There are three main programs which have conducted out-reactor tests on fission product release at: the Oak Ridge National Laboratories (ORNL) in the US, the Centre d'Études Nucléaire de Grenoble (CENG) in France, and the Chalk River Laboratories (CRL) of Atomic Energy of Canada Limited (AECL). The experimental apparatus and approach to fission product measurement has varied at the three sites. The following is a brief description of the results of the three programs with comments on the usefulness of the data.

3.1. ORNL experiments

The major recent ORNL tests are in the HI and VI series [26,29] Conditions for these tests and important test results are summarized in Tables 1 and 2. Both test series used highly-irradiated Zircaloy-clad UO_2 fuel samples that were 15–20 cm long (100–200 g). In these tests, fuel specimens have been heated under atmospheric-pressure conditions at temperatures up to 1700–2700 K using induction furnaces; times at test temperatures were varied from 2–60 min. Major differences in the VI and HI tests were that: (i) the VI tests had the test sample oriented vertically (all other ORNL tests had horizontally oriented samples); (ii) the fuel burnups in the VI tests were for the most part higher than those used in the HI tests; and (iii) VI test temperatures (2300–2700 K) were higher than HI test temperatures (1675–2275 K). The VI-3, VI-5 and VI-6 tests were performed at maximum test temperatures of approximately 2700 K; the test atmosphere (steam in VI-3, hydrogen in VI-5, hydrogen followed by steam in VI-6, air and steam in VI-7) was varied so that the influence of atmosphere on high-temperature fission product release could be evaluated.

Measurements made in the HI and VI tests included: (i) test sample temperature versus time by optical pyrometry; (ii) thermal gradient tube measurements downstream of the fuel sample, to collect condensing vapours; (iii) a package of graduated filters and impregnated charcoal cartridges to collect particulates and volatile iodine species; (iv) a charcoal cold trap to collect and measure fission gases; and (v) radiation detector measurements to monitor fuel location and to provide on-line measurements of cesium species in the thermal gradient tubes and Kr-85 in the gas traps. In addition, all test components were sampled and analyzed (by gamma-ray spectrometry, neutron activation analysis, spark-source mass spectrometry, and emission spectrometry) after each test.

Some of the key findings include confirmation of the similar release rates for noble gases, Cs and I. A difference in transport behaviour was noted for Cs in steam relative to hydrogen. Reactive vapour forms of Cs predominate in hydrogen conditions and transportable aerosols were noted in steam conditions. The releases of Te and Sb appear to occur from the UO_2 as for a volatile fission product, but these elements are retained by metallic Zircaloy, so their release is delayed until cladding oxidation is nearly complete (see Section 2.5.3). Both Eu and Sb showed a sensitivity to the oxygen potential at high temperatures [29]. Sb release rates were observed to increase in steam conditions relative to hydrogen at higher temperatures while hydrogen-rich conditions

Table 1
ORNL HI-series test conditions and results

Test characteristic	Test number					
	HI-1	HI-2	HI-3	HI-4	HI-5	HI-6
Specimen source, reactor [a]	HBR	HBR	HBR	PB	Oco	Mont
Specimen length (mm)	203	203	203	203	152	152
Specimen mass [b] (g)	168	166	167	306	133	170
Fuel burnup (GWd/Mg U)	28.1	28.1	25.2	10.1	38.3	40.3
In-pile gas release	0.3	0.3	0.3	10.2	4.1	2.0
Steam flow rate (g/h)	0.81	0.76	0.31	0.29	0.03	1.7 [c]
Test heatup rate (K/s)	1.2	1.3	2.1	2.3	1.1	2.3
Test temperature (K)	1675	2000	2275	2200	2025	2250
Effective time at test temperature [d] (min)	33.8	22.5	21.3	21.6	21.5	2.5
UO_2 grain size (μm)						
Pre-test	2.8	2.8	2.8	6.6	9.2	–
Post-test	3.4	3.9	4.3	6.6	8.9	
Fuel–cladding interaction	None	Minor	Yes	Yes	Minor	Yes
Fission Product Release (% of inventory)						
Kr-85 [e]	3.13	51.8	59.3	31.3	19.9	31.6
I-129	2.04	53.0	35.4	24.7	22.4	24.7
Cs- 137	1.75	50.5	58.8	31.7	20.3	33.1
Ag-110m[f]	∼0.3	2.9	0.02	>0.09	18.0	6.0
Sb-125 [g]	0.02	1.55	>0.001	0.01	0.33	0.06
Te (elemental) [h]	∼0.25	∼0.5	∼0.3	<0.4	–	–
Ba	∼0.008	–	–	<0.4	∼0.08	–
Sr	<0.002		–	<0.005	–	–
Eu-154	–	–	–	<0.6	∼0.02	–
Mo	–	∼5.9	–	–	–	–
Sn (clad)	–	–	∼1.7	∼1.1	∼0.5	–
Zr (clad)	∼0.006	∼0.002	∼0.0001	∼0.0016	–	–
La	∼0.023	–	<0.0002	–	–	–

[a] Reactors: HBR = H.B. Robinson 2, PB = Peach Bottom 2, Oco = Oconee 1, Mont = Monticello.
[b] Total of UO_2 and Zircaloy.
[c] Average value over test time (rate varied from 0.2 to 2.4 g/min during test).
[d] Includes estimates for heatup and cooldown effects.
[e] Includes Kr-85 released during reactor operation.
[f] Ag-110 m data for tests HI-2 through HI-4 are probably low.
[g] Sb-125 data are probably low for all tests.
[h] Determined by chemical analysis.

caused higher releases of Eu compared with steam environments [41].

There was limited on-line measurement of fission product release rates (only Cs-137 and Kr-85) in these experiments. Since a segmented furnace tube was used in the tests (to allow for rapid heating), there was not good containment of the test environment. There is evidence of oxidation of the graphite susceptor in some of the tests [24]. In most of the tests the samples were at temperature for a relatively short period of time (about 20 min), i.e., this time may not have been long enough to see oxidative releases (especially in the tests at lower temperature).

3.2. *CEN-grenoble experiments*

Fission-product and structural material releases from PWR fuel specimens have been studied in out-reactor experiments by the French CEA at Grenoble [24,35,40,107,131]. The HEVA program was conducted between 1983 and 1989, and consisted of 8 tests in the temperature range 1800–2370 K. An induction furnace was used to heat Zircaloy-clad specimens of PWR fuel, and gamma spectrometry was used to measure the fission product releases from the fuel and transport to different locations in the apparatus. In most of the tests, aerosols were collected in a heated cascade impactor and

Table 2
Conditions and results for ORNL VI-series fission product release tests

Parameter	Test number						
	VI-1	VI-2	VI-3	VI-4	VI-5	VI-6	VI-7
Fuel specimen	Oconee	BR3	BR3	BR3	BR3	BR3	Monticello
Burnup (GWd/MgU)	40	44	44	47	42	42	40
In-pile Kr release (%)	0.7	≈2	≈2	≈5	≈2	≈2	≈2
Test conditions							
Test temperature (K)	2020,2300 [a]	2300	2000,2700 [a]	2440	2000,2720 [a]	2310	2025,2310 [a]
Time at temperature (min)	20,20	60	20,50	20	20,20	60	20,20
Atmosphere	Steam	Steam	Steam	Steam	Hydorgen	Hydrogen, steam [c]	Air, steam
Fractional release (%)							
Cs-137	63	67	100	96	100	80	71
Kr-85	57	31	100	85	100	75	69
I-129	37	33	[b]	71	74	67	[b]
Sb-125	33	68	99	6.4	18	64	52
Eu-154	0	0	∼0.01	19	57	14	0.04
Ru-106	0	0	5.0	0	0	0	[b]
Te (elemental)	–	–	99	–	82	63	–
Sr (elemental)	–	–	3	–	34	6	1
Ba (elemental)	–	19	30	27	76	33	4
Sn (clad)	–	94	76	0.63	–	–	–
Mo (elemental)	43	86	77	6.9	2.3	12.6	–
Ce-144	–	–	<0.2	–	2.0	–	–

[a] Test was conducted in two phases at two different temperatures.

[b] Analysis incomplete.

[c] Test VI-6 was heated at 2300 K in hydrogen, then switched to a steam atmosphere.

in filters. Control rod materials were used in the last two tests (HEVA-07 with Ag–In–Cd exclusively and HEVA-08 with both control rods and fuel). Mixtures of steam/H_2 and pure H_2 have been used as the environments for the HEVA tests. Table 3 summarizes the HEVA test conditions and fission product release results.

The VERCORS program is an ongoing extension of the HEVA tests using a modified apparatus with augmented instrumentation. To-date, six tests have been completed in this program, up to a maximum temperature of 2350°C. Extensive post-test gamma scanning (including gamma tomography) has been done after the VERCORS tests. Most of the more recent tests in the HEVA–VERCORS program have used spent PWR fuel that was re-irradiated in the SILOE research reactor, after a period of decay following discharge from a power reactor. This permits the detection of short-lived fission products such as I, Te, Mo, Ba and La. Test conditions and results from the VERCORS test series are shown in Table 4.

The post-test gamma scanning done in these experiments enable a complete fission product mass balance to be conducted. However, there have been similar problems to the ones at ORNL in the control of the environment where there is no on-line measurement of the atmosphere (i.e., oxygen potential) during the tests.

3.3. CRL experiments

Six different types of furnaces have been used in experiments at CRL, depending on the temperature range and size of specimen to be heated. For all experiments, monitoring and control of the gas environment have been a priority; in particular, control of the oxygen potential to which the fuel is exposed. One of the key features of the AECL program has been on-line measurement of the oxygen potential in the gas stream, which allows for the fuel oxidation kinetics to be calculated [132]. Another key feature of these tests has been a direct measurement of the fission-product release rates, using a gamma-ray spectrometer which views the heated specimen through a collimated aperture [133]. A second spectrometer is used to monitor activity in the exhaust gas swept out of the furnace [134].

The fuel specimens include UO_2 fragments (0.2–1.5 g each) that were extracted from irradiated fuel elements after discharge and subsequent cutting. These tests have provided information on fission-product release from

Table 3
Conditions and results for CEA grenoble HEVA tests

Parameter	Test number							
	HEVA 01	HEVA 02	HEVA 03	HEVA 04	HEVA 05	HEVA 06	HEVA 07	HEVA 08
Fuel specimen								
Fuel type	CAP/2	CAP/2	BR3	Fessenheim 1/2	Fessenheim 1/2	Fessenheim 1/2		Fessenheim 1/2
Burnup (MWd/kgU)	19.4	19.4	27.7	36.7	36.7	36.7		36.7
Test conditions								
Test temperature plateau (K)	1900	2140	2070	2270	2070	2370	2070	2070
Time at temperature plateau (s)	900	900	1800	420	5760	1800	1800	600
Flow rate (mg/s)								
H_2	0	0	0.5	0.5	0.5	0.2	0.5	0.5
H_2O	100	30	37	30	30	0	25	25
Fractional release (%)								
Cs-137	~2	68	38	44	66	30	–	15
I-131	–	–	–	43	62	30	–	12
Xe-135	–	–	–	~42	~65	15	–	–
Te-132	–	–	–	52	54	11	–	5 (detection limit)
Sb-125	1	41	20	18	–	0 (Sb-127)	–	15 (detection limit)
Mo-99	–	–	–	21	55	~4	–	16 (detection limit)
Eu-154	–	~15	<3	–	–	~5	–	–
Ce-144	–	9 (detection limit)	<3.2	–	–	0 (Ce-143)	–	–
Ru-106	–	5 (detection limit)	<1.5	–	–	0 (Ru-103)	–	–
Ba-140	–	–	–	5.6	–	27	–	6 (detection limit)

bare UO_2 without any Zircaloy barrier. The role of Zircaloy on fission-product release has been investigated using fragments of UO_2 enclosed in Zircaloy foil bags, and short segments of Zircaloy-clad fuel elements with end caps fitted onto one or both ends of these samples to exclude the surrounding atmosphere from direct contact with the UO_2.

Experiments have been done on UO_2 fragments in steam, air and inert environments to temperatures up to 2350 K [135,136]. In total over 150 tests have been conducted on fragments of irradiated fuel [137]. About 40 tests have been conducted with Zircaloy-clad fuel segments to temperatures up to 2200 K. It has been shown that the presence of the Zircaloy sheath can either inhibit or delay the release of volatile fission products, compared to tests under the same conditions using bare UO_2. The delay is primarily associated with the time required to oxidize the Zircaloy cladding, after which the UO_2 begins to oxidize and cause enhanced release rates. Table 5 summarizes the test conditions and key results from a selected number of CRL tests. In more recent experiments with Zircaloy-clad segments, in addition to release from the fuel, deposition and transport of fission products have been studied. It is planned to do experiments in hydrogen-rich environments in the future.

Since the oxygen potential of the environment is known in the CRL tests, it has been possible to develop models for steam and air oxidation of UO_2 [24,73,74]. Enhanced release of Xe, Kr, Cs, and I have been observed during oxidation. Significant release of fission products such as Ru and Nb have been observed only in oxidizing environments and after the UO_2 has oxidized to an equilibrium state [62]. As well, the volatilization of the fuel matrix in oxidizing conditions has been modelled and identified as an important release mechanism for low-volatile fission products (e.g., Zr, La, Ba, Ce, Pr, Eu) in highly oxidizing environments or small fragments [42,135,137].

Table 4
Conditions and results for CEA grenoble VERCORS tests [a]

Parameter	Test number					
	VERCORS 01	VERCORS 02	VERCORS 03	VERCORS 04	VERCORS 05	VERCORS 06
Fuel specimen						
Burnup (MWd/kgU)	42.9	38.3	38.3	38.3	38.3	54.8
Reirradiation	Yes	Yes	Yes	Yes	Yes	Yes
Test conditions						
Test temperature plateau (K)	2130	2150	2570	2570	2570	2620
Time at temperature plateau (min)	17	13	15	30	30	30
Flow rate (g/min)						
H_2	0.003	0.003–0.027	0.03	0.012	0.03–0	0.03
H_2O	0.15	0.15–1.5	1.5	0	1.5	1.5
Heat rate (K/s)	1	1	1	1	1	1
Fractional release (%)						
Xenon	33	23	77	86		
Iodine	30	23	70	87		
Cesium	42	30	70	93		
Tellurium	4	18	76	100		
Antimony	2	7	69	97		
Molybdenum		15	42	47		
Barium	4	4	13	66		
Rhodium			0.52	45		
Yttrium			17			
Strontium			0	<8		
Europium			9	<5		
Ruthenium			0.36	7		
Cerium			0	3		
Neptunium	0.006	0.016	0.4	6		
Lanthanum			<4	0		
Zirconium			0	0		

[a] Taken from Ref. [40]

4. Concluding remarks

A review of important fission product release mechanisms has been presented. These mechanisms include: (i) diffusion in stoichiometric and non-stoichiometric fuel; (ii) fission product vaporization from fuel surfaces; (iii) releases during temperature ramps; (iv) matrix stripping; and (v) influence of the Zircaloy cladding (i.e., fuel dissolution by molten Zircaloy, chemical trapping, oxygen potential effects and gap transport). For example, these mechanisms have been observed in a number of experimental results of the out-of-pile annealing experiments performed with spent fuel at the ORNL (USA), CEA-Grenoble (France) and CRL (Canada).

In particular, enhanced releases have been observed from bare fuel fragments in the CRL tests due to fuel oxidation effects. The CRL experiments have shown that hydrogen production from the Zircaloy steam reaction will significantly reduce the oxygen potential and volatile release. Even with the presence of an oxidized Zircaloy cladding, a further reduction of the oxygen potential in the fuel-to-clad gap can result as steam must diffuse against a counter-current flow of non-condensible fission gas and any hydrogen that is produced from urania oxidation. A significant difference in the release behaviour was not observed, however, between the hydrogen and ‘steam’ tests at the ORNL and CEA since the oxygen potential was reduced due to significant steam bypass at both facilities. In these latter experiments, additional hydrogen was liberated from a steam reaction with the graphite susceptor of the furnace assembly. The various annealing experiments further demonstrated that the release of low-volatile fission products will be dictated by the local environmental conditions (i.e.,

Table 5
Conditions and results for selected CRL tests

Parameter	Test name							
	MCE1-1	MCE1-6	MCE1-7	MCE2-13	MCE2-19	HCE2-BM3	HCE2-CM4	UCE12-8
Fuel specimen	Fragment [a]	Fragment	Fragment	Fragment	Fragment	Segment[c]	Segment	Segment
Burnup (MWh/kgU)	257	257	257	457	457	544	457	370
Test conditions								
Test temperature (K)	1973	2273	2350	2080	2300	1775	1625	1675
Time at temperature (min)	13	37	17	17	10	110	140	200
Heating rate (K/s)	0.2	0.2	0.2	0.2	0.2	0.1	0.1	0.9
Atmosphere	Air	Ar/2%H2	Air	Steam	Steam	Steam	Air	Steam
Releases (%)								
Cs-137	80	80	100	92	100	75	75	96
I-131	80	80	100	NA	NA	NA	NA	NA
Nb-95	0	10	45	25	47	<2	3	<1
Zr-95	0	0	30	<2	<2	<2	<1	<1
Ru-103	100	1.0	100	NA	NA	NA	NA	NA
Ru-106	NA [b]	NA	NA	42	80	<2	20	<1
Ba-140	0	40	90	NA	NA	NA	NA	NA
La-140	0	0	35	NA	NA	NA	NA	NA
Ce-144	NA	NA	NA	<5	20	<2	<2	<2

[a] Bare fragment of UO_2.

[b] Isotope was not present in fuel at time of test.

[c] Zircaloy sheathed segment of a fuel element (2–5 cm long).

oxygen potential) which will directly influence their chemical form and hence the partial pressure of the fission product at the free surfaces of the fuel. Chemical reaction of some fission product vapours (e.g., tellurium) with the unoxidized Zircaloy cladding can also modify their release kinetics.

Direct electrical heating and out-of-pile experiments have indicated that the temperature ramp rate during a temperature transient can enhance the release behaviour. The mechanisms for such release include accelerated bubble interconnection and, with higher ramp rates (~50°C/s), a separation of the grain boundaries.

In both the CRL and CEA fuel oxidation experiments in steam, significant fuel volatilization occurred above about 1800 K where the principal form of the uranium bearing species is UO_3. Any volatile fission products originally present in this volatilized uranium mass will be released in this matrix stripping process.

Contact of the fuel with the Zircaloy cladding can result in fuel liquefaction at temperatures significantly below the UO_2 melting temperature. With the presence of molten Zircaloy, dissolution of the fuel can further result. Although fuel collapse has been observed in several ORNL VI hydrogen tests following clad melt and relocation, fuel dissolution did not result in a significantly enhanced fission product release. This observation follows since most of the release has already occurred by the time of dissolution, and any subsequent release of volatile fission gases from the dissolved fuel may be retarded by bubble dynamics in the liquid melt. In fact, the retarding influence of the bubble dynamics can lead to fuel frothing, where a resulting volume increase can impact the accessibility of coolant to the fuel.

References

[1] H. Kleykamp, J. Nucl. Mater. 131 (1985) 221.

[2] C.A. Friskney, M.V. Speight, J. Nucl. Mater. 62 (1976) 89.

[3] C.A. Friskney, J.A. Turnbull, J. Nucl. Mater. 79 (1979) 184.

[4] J.A. Turnbull, C.A. Friskney, J.R. Findlay, F.A. Johnson, A.J. Walter, J. Nucl. Mater. 107 (1982) 168.

[5] J.A. Turnbull, R.J. White, C. Wise, The diffusion coefficient for fission gas atoms in uranium dioxide, in: Proceedings of the International Atomic Energy Agency Technical Committee Meeting on Water Reactor Fuel Element Computer Modelling in Steady State, Transient and Accident Conditions, Preston, England, 18–22 September 1988.

[6] I.J. Hastings, C.E.L. Hunt, J.J. Lipsett, J. Nucl. Mater. 130 (1985) 407.

[7] B.J. Lewis, C.E.L. Hunt, F.C. Iglesias, J. Nucl. Mater. 172 (1990) 197.

[8] A.D. Appelhans, J.A. Turnbull, Measured release of radioactive xenon, krypton, and iodine from UO_2 at typical light water reactor conditions, and a comparison

with release models, Report NUREG/CR2298, US Nuclear Regulatory Commission, 1981.
[9] I. Ursu, C. Gheorghiu, C. Soare, E. Gheorghiu, Rev. Roum. Phys. Tome 32 (9) (1987) 951–960.
[10] H. Matzke, Adv. Ceram. 17 (1986) 1.
[11] C. Wise, J. Nucl. Mater. 136 (1985) 30.
[12] B.J. Lewis, J. Nucl. Mater. 148 (1987) 28.
[13] A.H. Booth, A suggested method for calculating the diffusion of radioactive rare gas fission products from UO_2 fuel elements and a discussion of proposed in-reactor experiments that may be used to test its validity, Atomic Energy of Canada Limited Report, AECL-700, 1957.
[14] G.V. Kidson, J. Nucl. Mater. 88 (1980) 299.
[15] B.J. Lewis, H.E. Sills, J. Nucl. Mater. 184 (1991) 107.
[16] R. Lindner, H. Matzke, Z. Naturforschg 14a (1959) 582.
[17] W. Miekeley, F. Felix, J. Nucl. Mater. 42 (1972) 297.
[18] G.T. Lawrence, J. Nucl. Mater. 71 (1978) 195.
[19] H. Matzke, Radiat. Eff. 53 (1980) 219.
[20] J.C. Killeen, J.A. Turnbull, An experimental and theoretical treatment of the release of Kr from hyperstoichiometric uranium dioxide, in: Proceedings of the Workshop Chemical Reactivity of Oxide Fuel and Fission Product Release, Gloucestershire, England, 7–9 April 1987, p. 387; Central Electricity Generating Board.
[21] R.W. Grimes, C.R. Catlow, Philos. Trans. R. Soc. Lond. A 335 (1991) 609.
[22] B.J. Lewis, F.C. Iglesias, D.S. Cox, E. Gheorghiu, Nucl. Technol. 92 (1990) 353.
[23] B.J. Lewis, D.S. Cox, F.C. Iglesias, J. Nucl. Mater. 207 (1993) 228.
[24] B.J. Lewis, B. Andre, B. Morel, P. Dehaudt, D. Maro, P.L. Purdy, D.S. Cox, F.C. Iglesias, M.F. Osborne, R.A. Lorenz, J. Nucl. Mater. 227 (1995) 83.
[25] S.G. Prussin, D.R. Olander, W.K. Lau, L. Hansson, J. Nucl. Mater. 154 (1988) 25.
[26] M.F. Osborne, J.L. Collins, R.A. Lorenz, Nucl. Technol. 78 (1987) 157.
[27] M.F. Osborne, R.A. Lorenz, J.L. Collins, T. Nakamura, Time-dependent release of fission products from LWR fuel under severe accident conditions, in: Proceedings of the International Conference on Thermal Reactor Safety, Avignon, France, 2–7 October, 1988, p. 1293.
[28] T.S. Kress, R.A. Lorenz, T. Nakamura, M.F. Osborne, Correlation of recent fission product release data, in: J.T. Rogers (Ed.), Fission Product Transport Processes in Reactor Accidents, Hemisphere, New York, 1990.
[29] M.F. Osborne, R.A. Lorenz, Nucl. Safety 33 (1992) 344.
[30] M. Peehs, G. Kaspar, K.H. Neeb, Cs and I source terms of irradiated UO_2, in: Proc. Topl. Mtg. Fission Product Behaviour and Source Term Research, Snowbird, Utah, 15–19 July 1984; Electric Power Research Institute, 1985.
[31] M. Peehs, G. Kaspar, F. Sontheimer, Cs and I source terms of irradiated UO_2, IAEA Technical Committee On Fuel Rod Internal Chemistry And Fission Product Behaviour, Karlsruhe, FRG, 11–15 November 1985, IWGFPT/25.
[32] G. Kaspar, M. Peehs, Transient release of iodine and cesium from irradiated UO_2 in presence of zircaloy and oxygen, Proc. Workshop Chemical Reactivity of Oxide Fuel and Fission, in: Product Release, Gloucestershire, England, 7–9 April 1987, p. 441; Central Electricity Generating Board.
[33] B.J. Lewis, F.C. Iglesias, C.E.L. Hunt, D.S. Cox, Nucl. Technol. 99 (1992) 330.
[34] A.C. Harnden-gillis, B.J. Lewis, W.S. Andrews, P.L. Purdy, M.F. Osborne, R.A. Lorenz, Nucl. Technol. 109 (1995) 39.
[35] B.J. Lewis, B. Andre, G. Ducros, D. Maro, Nucl. Technol. 116 (1996) 34.
[36] J. Rest, A.W. Cronenberg, J. Nucl. Mater. 150 (1987) 203.
[37] A.H. Booth, A method for calculating fission gas diffusion from UO_2 fuel and its application to the X-2-f loop test, Atomic Energy Of Canada Limited Report, AECL-496, 1957.
[38] B.J. Lewis, F.C. Iglesias, J. Nucl. Mater. 154 (1988) 228.
[39] M. Ramamurthi, M.R. Kuhlman, Refinement of CORSOR – An empirical in-vessel fission product release model, US Nuclear Regulatory Commission, Battelle report, 1990.
[40] B. Andre, G. Ducros, J.P. Leveque, M.F. Osborne, R.A. Lorenz, D. Maro, Nucl. Technol. 114 (1996) 23.
[41] R.A. Lorenz, M.F. Osborne, A summary of ORNL fission product release tests with recommended release rates and diffusion coefficients, NUREG/CR-6261, ORNL/TM-12801, July 1995.
[42] B.J. Lewis, B.J. Corse, W.T. Thompson, M.H. Kaye, F.C. Iglesias, P. Elder, R. Dickson, Z. Liu, J. Nucl. Mater. 252 (1998) 235.
[43] K. Une, S. Kashibe, J. Nucl. Mater. 189 (1992) 210.
[44] J. Rest, J. Nucl. Mater. 120 (1984) 195.
[45] J. Rest, J. Nucl. Mater. 131 (1985) 291.
[46] J. Rest, Adv. Ceram. 17 (1986) 223.
[47] J.R. Mathews, M.H. Wood, Nucl. Eng. Des. 56 (1980) 439.
[48] M.A. Mansouri, D.R. Olander, J. Nucl. Mater. 254 (1998) 22.
[49] J. Belle, B. Lustman, Properties of UO_2, WAPD-184, presented at Paris Fuel Technology Conference, 1957.
[50] J.T. Bittel, L.H. Sjohdal, J.F. White, J. Am. Ceram. Soc. 52 (8) (1968) 446.
[51] D.S. Cox, F.C. Iglesias, C.E.L. Hunt, N.A. Keller, R.D. Barrand, J.R. Mitchell, R.F. O'Connor, Oxidation of UO_2 in air and steam with relevance to fission product releases, in: Proceedings of the American Chemical Society Symposium on Chemical Phenomenon Associated with Radioactivity during Severe Nuclear Plant Accidents, Anaheim, California, 9–12 September 1986, NUREG/CP-0078, US Nuclear Regulatory Commission, pp. 2–35.
[52] R. Aboud, V.I. Nath, R. Hu, Modelling fission product releases due to UO_2 oxidation in a steam environment, in: Proceedings of the 16th Annual Nuclear Simulation Symposium, Canadian Nuclear Society, St. John, New Brunswick, 25–27 August 1992.
[53] A.B. Reynolds, J.L. Kelly, S.T. Kim, Nucl. Technol. 74 (1986) 76.
[54] D. Cubicciotti, Vaporization Thermodynamics Of Fission Products From Fuel Under Nuclear-Accident Conditions, Advances In Ceramics, vol. 17, American Ceramic Society, Columbus, Ohio, 1986, p. 211.
[55] D. Cubicciotti, B.R. Sehgal, Nucl. Technol. 65 (1984) 267.

[56] D. Cubicciotti, J. Nucl. Mater. 154 (1988) 53.

[57] E.H.P. Cordfunke, R.J.M. Konings, J. Nucl. Mater. 152 (1988) 301.

[58] J.M. Gittus, J.R. Matthews, P.E. Potter, J. Nucl. Mater. 166 (1989) 132.

[59] M.H. Kaye, W.T. Thompson, B.J. Lewis, Trans. Am. Nucl. Soc., Washington, DC 79 (1998) 123.

[60] R.R. Hobbins, D.A. Petti, D.L. Hagrman, Nucl. Technol. 101 (1993) 270.

[61] M.D. Allen, H.W. Stockman, K.O. Reil, A.J. Grimley, W.J. Camp, ACRR fission product release tests ST-1 and ST-2, in: Proceedings of the International Conference on Thermal Reactor Safety, vol. 5, Avignon, France, 2–7 October 1988.

[62] F.C. Iglesias, C.E.L. Hunt, F. Garisto, D.S. Cox, Ruthenium release kinetics from uranium oxides, in: Proceedings of the ICHMT Conference on Fission Product Transport Processes in Reactor Accidents, Dubrovnik, Yugoslavia, 22–26 May 1989, Hemisphere, New York, 1990, pp. 187–196.

[63] F. Garisto, Thermodynamic behaviour of ruthenium at high temperatures, Atomic Energy of Canada Limited report, AECL-9552, 1988.

[64] M. Sontheimer, R. Manzel, H. Stehle, J. Nucl. Mater. 124 (1984) 33.

[65] J. Rest, S.M. Gehl, Nucl. Eng. Design 56 (1980) 233.

[66] S. Kashibe, K. Une, J. Nucl. Sci. Technol. 28 (1991) 1090.

[67] K. Une, S. Kashibe, J. Nucl. Mater. 189 (1992) 210.

[68] G.J. Small, Fission gas release and bubble development in UO_2 during high temperature transients, in: Proceedings of the IAEA Specialist Meeting on Water Reactor Fuel Element Computer Modelling in Steady State, Transient and Accident Conditions, Preston, 1988.

[69] J.R. Mathews, G.J. Small, Towards a mechanistic understanding of transient fission gas release, in: Proceedings of the IAEA Specialist Meeting on Water Reactor Fuel Element Computer Modelling in Steady State, Transient and Accident Conditions, Preston, 1988.

[70] P.L. Purdy, B.J. Lewis, W.S. Andrews, D.S. Cox, F.C. Iglesias, A model for fuel oxidation and diffusion-based fission product release under severe nuclear reactor accident conditions, in: Fourth International Conference on CANDU Fuel, Pembroke, Ontario, 1–4 October 1995.

[71] C.A. Alexander, J.S. Ogden, L. Chan, R.W. Wright, Matrix stripping and fission product release at high temperature, in: Proceedings of the IAEA/OECD International Symposium on Severe Accidents in Nuclear Power Plants, Sorrento, Italy, 21–25 March 1988 (IAEA-SM-296/99).

[72] C.A. Alexander, J.S. Ogden, High Temp. High Press. 21 (1990) 149.

[73] D.S. Cox, C.E.L. Hunt, R.F. O'Connor, R.D. Barrand, F.C. Iglesias, High temperature oxidation behaviour of UO_2 in air and steam, in: Proceedings of the International Symposium on High Temperature Oxidation and Sulphidation Process, Hamilton, Ontario, Canada, 26–30 August 1990, Pergamon Press, New York, ISBN 0-18-040415-4.

[74] D.S. Cox, C.E.L. Hunt, Z. Liu, F.C. Iglesias, N.A. Keller, R.D. Barrand, R.F. O'Connor, A model for the release of low-volatility fission products in oxidizing conditions, Atomic Energy of Canada Limited report, AECL-10440, July 1991.

[75] D.R. Olander, these Proceedings, p. 187.

[76] T.J. Heames, D.A. Williams, N.E. Bixler, A.J. Grimley, C.J. Wheatley, N.A. Johns, P. Domagala, L.W. Dickson, C.A. Alexander, I. Osborn-Lee, S. Zawadzki, J. Rest, A. Mason, R.Y. Lee, VICTORIA: A Mechanistic Model of Radionuclide Behaviour in the Reactor Coolant System Under Severe Accident Conditions, US Nuclear Regulatory Commission, NUREG/CR-5545, SAND90-0756, Rev. 1, R3, R4, December 1992.

[77] R.J. Ackermann, A.T. Chang, J. Chem. Thermo. 5 (1973) 873.

[78] E.H.P. Cordfunke, R.J.M. Konings (Eds.), Thermochemical Data for Reactor Materials and Fission Products, North Holland, Amsterdam, 1990.

[79] O.H. Krikorian et al., Experimental studies and thermodynamic modeling of volatilities of uranium, plutonium, and americium from their oxides, Lawrence Livermore National Laboratory report, UCRL-ID-114774, 1993.

[80] B.B. Ebbinghaus, Calculated Thermodynamic Functions for Gas-phase Uranium, Neptunium, Plutonium, and Americium Oxides, Oxyhydrioxides, Oxychlorides, and Oxyfluorides, Lawrence Livermore National Laboratory report, UCRL-JC-122278, 1995.

[81] B.B. Ebbinghaus, O.H. Krikorian, D.L. Fleming, Thermodynamic Study of $UO_3(g)$, $UO_2(OH)_2$, $UO_2Cl_2(g)$ and $UO_2F_2(g)$, Lawrence Livermore National Laboratory unpublished manuscript, 1995.

[82] V. Ozrin et al., Models for Release of Low-volatile Fission Products, Institute of Russian Academy of Sciences, NSI-SARR-43-96, 1996.

[83] H. Manenc, M.J. Notley, ELSA: A simplified code for fission product release calculations, Transactions of the American Nuclear Society, 1996 International Conference on the Global Benefits of Nuclear Technology, 10–14 November, 1996, ISSN 0003-018X, p. 250, American Nuclear Society, La Grange Park, IL, 1996.

[84] W. Dienst, P. Hofmann, D. Kerwin-Peck, Nucl. Technol. 65 (1984) 109.

[85] A.R. Paul, M.C. Naik, K.S. Venkateswariu, Kinetics of Interfacial Reaction Between Uranium Dioxide and Zircaloy-2, Bhaba Atomic Research Centre report 1087, 1980.

[86] H.E. Rosinger, A Study of the Pellet/Clad (Uranium Dioxide/Zircaloy-4) Interaction at 1373 and 1473 K, Atomic Energy of Canada Limited report, AECL-7785, February 1983.

[87] R.V. Strain, Proc. Top. Mtg. Fission Product Behavior and Source Term Research, Snowbird, UT, 1983, American Nuclear Society, Lagrange Park, IL, 1984, p. 2.1.

[88] P. Hofmann, H. Uetsuka, A.N. Wilhelm, E.A. Garcia, in: Proceedings of the IAEA/OECD International Symposium on Severe Accidents in Nuclear Power Plants, Sorrento, Italy, 21–25 March 1988 (IAEA-SM-296/99), p. 3.

[89] P. Nikolopoulos, P. Hofmann, D. Kerwin-Peck, J. Nucl. Mater. 124 (1984) 106.

[90] K.Y. Kim, D.R. Olander, J. Nucl. Mater. 154 (1988) 85.

[91] H.E. Rosinger, K. Demoline, R.K. Rondeau, The dissolution of UO_2 by molten zircaloy-4 cladding, in: Pro-

ceedings of the Fifth International Meeting on Thermal Nuclear Reactor Safety, Karlsruhe, FRG, September 1984. Also published as Atomic Energy of Canada Limited report, AECL-8387, March 1985.

[92] P.J. Hayward, I.M. George, J. Nucl. Mater. 208 (1994) 35.

[93] P.J. Hayward, I.M. George, J. Nucl. Mater. 208 (1994) 43.

[94] P.J. Hayward, I.M. George, J. Nucl. Mater. 232 (1996) 1.

[95] P.J. Hayward, I.M. George, J. Nucl. Mater. 232 (1996) 13.

[96] A. Wilhelm, E. Garcia, J. Nucl. Mater. 158 (1988) 143.

[97] M.S. Veshchunov, A.M. Volchek, J. Nucl. Mater. 188 (1992) 177.

[98] D.R. Olander, Materials-Chemistry and Transport Modeling for Severe Accident Analysis in Light Water Reactors, Lawrence Berkeley Laboratory report, LBL-32530, 1992.

[99] M.S. Veshchunov, P. Hofmann, J. Nucl. Mater. 209 (1994) 27.

[100] D.R. Olander, J. Nucl. Mater. 224 (1995) 254.

[101] M.S. Veshchunov, P. Hofmann, A.V. Berdyshev, J. Nucl. Mater. 231 (1996) 1.

[102] P.J. Hayward, I.M. George, R.A. Kaatz, D.R. Olander, J. Nucl. Mater. 244 (1997) 36.

[103] M.D. Allen, H.W. Stockman, K.O. Reil, Fission product release and fuel behavior of irradiated light water reactor fuel under severe accident conditions: The ACRR ST-1 experiment, SAND89-0308, NUREG/CR-5345, September 1991.

[104] M.D. Allen, H.W. Stockman, K.O. Reil, A.J. Grimley, Nucl. Technol. 92 (1990) 214.

[105] M.F. Osborne, R.A. Lorenz, J.L. Collins, J.R. Tracis, C.S. Webster, T. Nakamura, Data Summary Report for Fission Product Release Test VI-4, ORNL/TM-11400, NUREG/CR-5481, January 1991.

[106] J.L. Collins, M.F. Osborne, R.A. Lorenz, Nucl. Technol. 77 (1987) 18.

[107] J.P. Leveque, G. Lhiaubet, B. Boulaud, HEVA Experimental programme: Final Report, Commissariat á l''Energie Atomique report, DPEI/SEAC No. 91/08, November 1991.

[108] I. Johnson, C.E. Johnson, J. Nucl. Mater. 154 (1988) 67.

[109] B.R. Bowsher, S. Dickinson, R.A. Gomme, R.A. Jenkins, A.L. Nichols, J.S. Ogden, The interaction of Zircaloy cladding with fission product tellurium released during a severe reactor accident, in: Proceedings of the Workshop Chemical Reactivity of Oxide Fuel and Fission Product Release, Gloucestershire, England, 7–9 April 1987; Central Electricity Generating Board, p. 455.

[110] R. De Boer, E.H.P. Cordfunke, J. Nucl. Mater. 223 (1995) 103.

[111] R. De Boer, E.H.P. Cordfunke, J. Nucl. Mater. 240 (1997) 124.

[112] B.J. Lewis, H.W. Bonin, J. Nucl. Mater. 218 (1994) 42.

[113] Z.W. Lian, L.N. Carlucci, V.I. Arimescu, Convective-diffusive transport of fission products in the gap of a failed fuel element, Proceedings of the 15th Annual Conference of the Canadian Nuclear Society, Canadian Nuclear Society, Session 5C, Montreal, Quebec, 5–8 June 1994.

[114] H.W. Bonin, B.J. Lewis, Simulation of the transport of volatile fission products within the fuel-to-sheath gap of defective CANDU fuel rods, in: Proceedings of the Fifth International Conference on CANDU Fuel, ISBN 0-919784-48-8, Toronto, Ontario, 21–24 September 1997, pp. 118–132.

[115] D.R. Olander, Nucl. Eng. Des. 148 (1994) 273.

[116] B.J. Lewis, these Proceedings, p. 221.

[117] Z. Liu, P.H. Elder, R.S. Dickson, S.T. Craig, High-Temperature Fission Product Release Measurement, unpublished .

[118] V. Mubayi, J.A. Gieseke, D.R. Olander, M. Schwarz, Victoria Independent Peer Review, Brookhaven National Laboratory report, W-6426, 17 April 1997.

[119] D.R. Olander, Nucl. Eng. Des. 148 (1994) 253.

[120] F.C. Iglesias, D.B. Duncan, S. Sagat, H.E. Sills, J. Nucl. Mater. 130 (1985) 36.

[121] M. Moalem, D.R. Olander, J. Nucl. Mater. 182 (1991) 170.

[122] M.H. Rand, R.J. Ackerman, F. Gronwold, F.L. Oetting, A. Pattoret, Rev. Int. Hautes Temp. Refract. 15 (1978) 355.

[123] R.E. Latta, R.E. Fryxell, J. Nucl. Mater. 35 (1970) 192.

[124] M.G. Adamson, E.A. Aitken, R.W. Caputi, J. Nucl. Mater. 130 (1985) 349.

[125] M. Koizumi, M. Satoh, J. Nucl. Mater. 51 (1974) 90.

[126] D.R. Boyle, F.L. Brown, J.E. Sanecki, J. Nucl. Mater. 29 (1968) 27.

[127] L.F. Epstein, J. Nucl. Mater 22 (1972) 340.

[128] A.W. Cronenberg, D.W. Croucher, P.E. Macdonald, Nucl. Technol. 67 (1984) 312.

[129] M.F. Osborne, J.L. Collins, R.A. Lorenz, J.R. Travis, C.S. Webster, Data Summary Report for Fission Product Release Test VI-2, ORNL/TM-11105, NUREG/CR-5340, September 1989.

[130] R.D. Macdonald, J.W. Devaal, D.S. Cox, L.W. Dickson, M.J. Jonckheere, C.E. Ferris, N.A. Keller, S.L. Wadsworth, An in-reactor loss-of-coolant test with flow blockage and rewet, in: Proceedings of the International Topical Meeting on Thermal Reactor Safety, Portland, Oregon, July 1991. Also issued as Atomic Energy of Canada Limited report, AECL-10464, October 1991.

[131] J.P. Leveque, B. Andre, G. Ducros, G. Le Marois, G. Lhiaubet, Nucl. Technol. 188 (1994) 33.

[132] D.S. Cox, R.F. O'Connor, W.W. Smeltzer, Solid State Ionics 53–56 (1992) 238.

[133] C.E.L. Hunt, F.C. Iglesias, D.S. Cox, N.A. Keller, R.D. Barrand, J.R. Mitchell, R.F. O'Connor, Fission product release during UO_2 oxidation, in: Proceedings of the International Conference on CANDU Fuel, Chalk River Nuclear Laboratories, Chalk River, Ontario, Canada, 6–8 October 1986, p. 508.

[134] D.S. Cox, Z. Liu, R.S. Dickson, P.H. Elder, Fission-product release during post-test annealing of high-burnup CANDU fuel, in: Proceedings of the Third International Conference on CANDU Fuel, Pembroke, Ont., Canada, 4–8 October 1992, pp. 4–61.

[135] D.S. Cox, C.E.L. Hunt, Z. Liu, N.A. Keller, R.D. Barrand, R.F. O'Connor, F.C. Iglesias, Fission-product releases from UO_2 in air and inert conditions at 1700–2350°K – Analysis of the MCE-1Experiment, in: Pro-

ceedings of the American Nuclear Society International Topical Meeting on Safety of Thermal Reactors, Portland, Oregon, USA, 21–25 July 1991. Also issued as Atomic Energy of Canada Limited report, AECL-10438.

[136] R.S. Dickson, Z. Liu, D.S. Cox, N.A. Keller, R.F. O'Connor, R.D. Barrand, Cesium release from CANDU fuel in argon, steam and air: The UCE12 experiment, in: Proceedings of the 15th Annual Canadian Nuclear Association Meeting, Montreal, Que., Canada, 1994.

[137] Z. Liu, D.S. Cox, R.S. Dickson, P. Elder, A Summary of CRL Fission-Product Release Measurements from UO_2 Samples During Post-Irradiation Annealing (1983–1992), COG-92-377, June 1994.